Conserved quantity of elastic waves in multi-layered media: 2D SH case -Normalized Energy Density-

Hiroyuki Goto[a,*], Sumio Sawada[a], Toshiyuki Hirai[b]

[a]*Disaster Prevention Research Institute, Kyoto University, Gokasho, Uji, Kyoto 611-0011, Japan*
[b]*NEWJEC Inc., 2-3-20 Honjo-Higashi, Kita-ku, Osaka 531-0074, Japan*

Abstract

We introduce a new conserved quantity, Normalized Energy Density (NED), alternative to the conventional definition of energy for a layered structure in a 2D SH problem. NED is defined by the average of power of a half transfer function multiplied by the impedance, and the conservation across the material interface is analytically proved for a two-layered case. For three, four, and ten-layered cases, the conservation is examined by applying the Monte Carlo simulation method, and then NED is supposed to be conserved through the layers.

Keywords: Elastic wave, Energy

1. Introduction

Conserved quantities, such as mass, momentum and energy, in elastodynamic problems are the fundamental variables when analyzing wave propagation in a continuous medium. In addition, the balance principles associated with these quantities, e.g., the balance of mass and the balance of momentum, govern the deformation within the framework of Newtonian mechanics. The balance of energy is one of the principles used to quantify the seismic energy radiated from an earthquake source.

*Corresponding author. Tel.:+81 774 38 4067; fax:+81 774 38 4070.
Email address: goto@catfish.dpri.kyoto-u.ac.jp (Hiroyuki Goto)

Radiation energy E is theoretically defined as the total energy transmitted through a certain surface, S, as follows:

$$E = -\int_0^\infty dt \int_S \left(\sigma_{ij} - \sigma_{ij}^0\right) \dot{u}_i n_j dS, \tag{1}$$

where σ_{ij} and σ_{ij}^0 are the tentative and the initial stress tensors, respectively. $\dot{u}_i$ is the particle velocity, and n_j is a normal vector of the surface S. When a particular region, e.g. a seismic fault, generates all of the energy, the integration on the arbitrary surface S surrounding the region is theoretically conserved even for a general heterogeneous medium. The above representation has already been introduced in Love [1] . The energy of seismic events was first applied by Richter [2] in order to measure the size of earthquakes by using the local magnitude scale (M_L), although it was not exactly equal to the definition of the energy. Afterward, Kanamori [3] proposed the use of moment magnitude (M_W), defined from the seismic moment that is related to the energy release during the events, whose energy is different from the radiation energy (Equation (1)). A detailed discussion on radiation energy is introduced in Kostrov and Das [4], Fukuyama [5], and Abercrombie et al. [6].

If a seismic wave through the surface S is approximated by a single plane wave, either a P- or an S-wave propagated in a uniform direction, the energy for the P-wave case, E_α, and that for the S-wave case, E_β, are represented as follows:

$$E_\alpha = \int_0^\infty dt \int_S \rho\alpha \dot{u}_\alpha^2 l_i n_i dS, \quad E_\beta = \int_0^\infty dt \int_S \rho\beta \dot{u}_\beta^2 l_i n_i dS, \tag{2}$$

where ρ, α and β are the density, the P-wave velocity, and the S-wave velocity, respectively. $\dot{u}_\alpha$ and $\dot{u}_\beta$ are the amplitudes of particle velocity for the P-wave and the S-wave, respectively. l_i is a vector representing the direction of the wave propagation. The energy density, defined by the integrand, is a product of the square of the particle velocity and the impedance. Note that the total energy for a general wave field, represented by the superposition of the P- and the S-waves, is not equal to $E_\alpha + E_\beta$ (see Appendix A).

A part of the energy integrated on the shrunken area of S is utilized as a principle of energy conservation when all of the input energy is confined in a certain region, so-called "ray tube" [7] . The energy on the cross-sectional area of the tube is theoretically conserved. Here, we focus on the layered

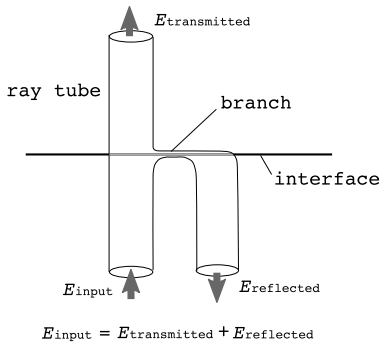

Figure 1: Ray tube at the material interface and the energy conservation.

structure. At the interface, part of the energy for the input wave is transmitted, and the rest is reflected. Then, both the transmitted and the reflected waves should be considered in order to apply the energy conservation in the ray tube. As shown in Figure 1, the sum of the transmitted energy and the reflected energy is equal to the input energy. However, the total input energy can not be observed in only the opposite layer because the transmitted energy is part of the input energy. Therefore, the energy is not conserved across the interfaces. Note that some researchers apply the energy, directly defined by $\int_0^\infty \rho c \dot{u}^2 dt$, to the layered structure (e.g., Kokusho and Motoyama [8]) , however, they do not pay attention to the fact that the quantity is not conserved. If a quantity conserved over the layer structure exists, absorbed energy in propagating in the layer might be estimated, directly. The quantification of the absorbed energy helps to understand the hysteretic damping due to anelasticity, e.g. Q-factor, and the soil nonlinearity, as discussed in Kokusho and Motoyama [8].

In this article, we introduce a quantity, Normalized Energy Density, which is an alternative to the conventional definition of energy, and discuss the features of the 2D SH problem. The quantity is analytically discussed for the two-layered case, and numerically examined for multi-layered cases.

2. Two-layered case

The theoretical implementation starts from the waves, vertically propagated into a simple two-layered structure. Only 2D SH waves, which have an antiplane amplitude with respect to the plane, are considered here. The structure consists of a horizontal layer, Layer #1, with a thickness of h and

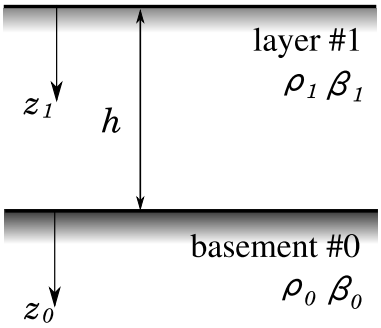

Figure 2: Two-layered model.

a half space basement, Basement #0. The S-wave velocity and the density are β_1 and ρ_1 for Layer #1 and β_0 and ρ_0 for Basement #0, as shown in Figure 2. An incident plane wave propagates vertically into Layer #1 through the interface between Layer #1 and Basement #0. Each layer keeps elasticity independent of the wave amplitude.

The displacement in each layer satisfies the following wave equations in the frequency domain:

$$-\frac{\omega^2}{\beta_1^2}\, u_1(\omega, z_1) = \frac{\partial^2 u_1(\omega, z_1)}{\partial {z_1}^2} \tag{3}$$

$$-\frac{\omega^2}{\beta_0^2}\, u_0(\omega, z_0) = \frac{\partial^2 u_0(\omega, z_0)}{\partial {z_0}^2}, \tag{4}$$

where ω is an angular frequency, and u_1 and u_0 are the displacements of Layer #1 and Basement #0, respectively. The general solutions for Equations (3) and (4) are represented by the superposition of upgoing and downgoing waves, namely,

$$u_1(\omega, z_1) = A_1 e^{i\omega z_1/\beta_1} + B_1 e^{-i\omega z_1/\beta_1} \tag{5}$$

$$u_0(\omega, z_0) = A_0 e^{i\omega z_0/\beta_0} + B_0 e^{-i\omega z_0/\beta_0}, \tag{6}$$

where i indicates an imaginary unit. A_1 and A_0 are the amplitudes of the upgoing waves, while B_1 and B_0 are those for the downgoing waves. The boundary conditions at the interface are as follows:

$$u_1(\omega, h) = u_0(\omega, 0), \quad \rho_1 \beta_1^2 \frac{\partial u_1}{\partial z_1}\bigg|_{z_1=h} = \rho_0 \beta_0^2 \frac{\partial u_0}{\partial z_0}\bigg|_{z_0=0}. \tag{7}$$

Then, the amplitudes for Basement #0 are represented by those for Layer #1 via the following matrix equation.

$$\begin{pmatrix} A_0 \\ B_0 \end{pmatrix} = \begin{bmatrix} \frac{1}{2}(1+R_{1,0})e^{i\omega h/\beta_1}, & \frac{1}{2}(1-R_{1,0})e^{-i\omega h/\beta_1} \\ \frac{1}{2}(1-R_{1,0})e^{i\omega h/\beta_1}, & \frac{1}{2}(1+R_{1,0})e^{-i\omega h/\beta_1} \end{bmatrix} \begin{pmatrix} A_1 \\ B_1 \end{pmatrix}, \tag{8}$$

where $R_{1,0}$ represents an impedance ratio ($= \rho_1\beta_1/\rho_0\beta_0$). Since the space differentiation of the displacement is zero on the free surface, the amplitude of an upgoing wave, A_1, should be equal to that of a downgoing wave, B_1. Then, the ratio, A_1/A_0, is represented by the following form:

$$\frac{A_1}{A_0} = \frac{1}{\cos(\omega h/\beta_1) + iR_{1,0}\sin(\omega h/\beta_1)}. \tag{9}$$

Quantity A_1/A_0 is half of transfer function $H(\omega)$, ratio of free surface displacement to input wave, for the two-layered structure,

$$H(\omega) \equiv \frac{u_1(\omega, 0)}{A_0} = \frac{2A_1}{A_0}. \tag{10}$$

Here, we define real functions P_1 and P_0 as the square of the absolute value of the upgoing wave amplitudes A_1 and A_0 normalized by input wave amplitude.

$$P_1(\omega) = \left|\frac{A_1}{A_0}\right|^2 = \frac{1}{\cos^2(\omega h/\beta_1) + {R_{1,0}}^2\sin^2(\omega h/\beta_1)}, \tag{11}$$

$$P_0(\omega) = \left|\frac{A_0}{A_0}\right|^2 = 1. \tag{12}$$

P_1 is a single-valued function with respect to $\cos(\omega h/\beta_1)$, and a periodic function of $\omega h/\beta_1 = n\pi$ ($n \in \mathbb{N}$). Moreover, P_1, defined in $\omega h/\beta_1 \in [0, \pi]$, is symmetric about $\pi/2$. Therefore, the average of P in $\omega \in [-\infty, \infty]$, defined by $\langle P_1 \rangle$, is equal to the average of P_1 in $\omega h/\beta_1 \in [0, \pi/2]$.

$$\begin{aligned} \langle P_1 \rangle &= \lim_{\Omega\to\infty} \frac{1}{\Omega} \int_{-\Omega/2}^{\Omega/2} \frac{1}{\cos^2(\omega h/\beta_1) + {R_{1,0}}^2\sin^2(\omega h/\beta_1)}\, d\omega \\ &= \frac{2}{\pi} \int_0^{\pi/2} \frac{d\tilde{\omega}}{\cos^2(\tilde{\omega}) + {R_{1,0}}^2\sin^2(\tilde{\omega})}, \end{aligned} \tag{13}$$

where $\tilde{\omega} = \omega h/\beta_1$. The above integration is analytically integrable, as follows:

$$\int_0^{\pi/2} \frac{d\tilde{\omega}}{\cos^2(\tilde{\omega}) + {R_{1,0}}^2 \sin^2(\tilde{\omega})} = \left[\frac{1}{R_{1,0}} \tan^{-1} \left(R_{1,0} \tan(\tilde{\omega}) \right) \right]_0^{\pi/2} = \frac{\pi}{2R_{1,0}}, \quad (14)$$

Thus, the average of P_1 is equal to the inverse of impedance ratio $R_{1,0}$.

$$\langle P_1 \rangle = \frac{1}{R_{1,0}} = \frac{\rho_0 \beta_0}{\rho_1 \beta_1}. \quad (15)$$

When the input wave satisfies $|A_0| = 1$, $\langle P_1 \rangle$ represents the average power for the upgoing waves in Layer #1 or for half the amplitude of the waves observed on the free surface. On the other hand, the average of P_0 is identical to 1 because of $P_0 = 1$.

$$\langle P_0 \rangle = 1. \quad (16)$$

We define a quantity, a product of the average of P and the impedance $\rho\beta$, such as $\rho_1\beta_1\langle P_1 \rangle$ for Layer #1 and $\rho_0\beta_0\langle P_0 \rangle$ for Basement #0. From the explicit representations of $\langle P_1 \rangle$ and $\langle P_0 \rangle$ by Eqs.(15)-(16), the following relation is obtained:

$$\rho_1\beta_1\langle P_1 \rangle = \rho_0\beta_0\langle P_0 \rangle. \quad (17)$$

Equation (17) includes some physical features. Both the left- and right-hand sides are the average power of the upgoing waves multiplied by the impedance at each layer. This means that the quantity, $\rho\beta\langle P \rangle$, is conserved across the interface. Moreover, the quantity is directly evaluated from the transfer function $H(\omega)$ as

$$\rho_1\beta_1\langle P_1 \rangle = \lim_{\Omega \to \infty} \frac{1}{\Omega} \int_{-\Omega/2}^{\Omega/2} \rho_1\beta_1 \left| \frac{H(\omega)}{2} \right|^2 d\omega. \quad (18)$$

Let $g(t)$ to be an impulse response in a time domain for the upgoing waves in Layer #1. Although $g(t)$ is not guaranteed to be a stationary ergodic process, the formally defined average power spectral density is generally equal to $\langle P_1 \rangle$. Since the average power spectral density for a stationary ergodic process is a variance of the process, the quantity may be formally defined as a product of the impedance $\rho_1\beta_1$ and the variance of $g(t)$, as follows:

$$\rho_1\beta_1\langle P_1 \rangle = \lim_{T \to \infty} \frac{1}{T} \int_{-T/2}^{T/2} \rho_1\beta_1 \left[g(t) - \langle g(t) \rangle \right]^2 dt, \quad (19)$$

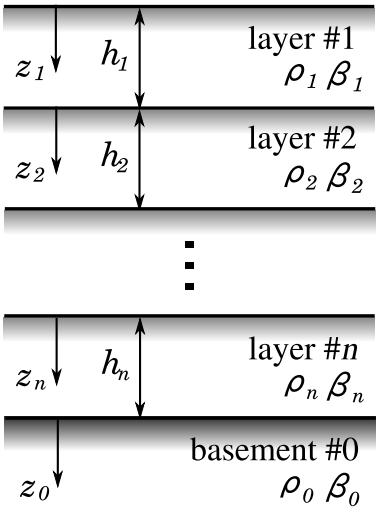

Figure 3: Multi-layered model.

where $\langle g(t) \rangle$ is the average $g(t)$. Note that the derivation of Equation (19) should be discussed after the treatment for the convergence of the integration, the super function, etc. We just mention that the representation of Equation (19) is similar to the conventional definition of the energy, whereas the proposed quantity, which is limited to the unity input waves, gives rise to conservation across the interface. Therefore, we name the quantity $\rho\beta\langle P \rangle$, Normalized Energy Density (NED).

3. Multi-layered case

We consider a multi-layered structure consisting of n layers (#1-#n) over Basement #0, as shown in Figure 3. The S-wave velocity of Layer #k is β_k, the density is ρ_k, and the thickness is h_k. 2D SH waves vertically propagate vertically into the layers through the interface between Layer #n and Basement #0.

The general solution for the wave equation at Layer #k is obtained by

$$u_k(\omega, z_k) = A_k e^{i\omega z_k/\beta_k} + B_k e^{-i\omega z_k/\beta_k}. \tag{20}$$

From the boundary conditions at the interface between Layers #$(k+1)$ and #k, the amplitudes for Layer #$(k+1)$ are represented by those for Layer

#k as

$$\begin{pmatrix} A_{k+1} \\ B_{k+1} \end{pmatrix} = \begin{bmatrix} \frac{1}{2}(1+R_{k,k+1})e^{i\omega h_k/\beta_k}, & \frac{1}{2}(1-R_{k,k+1})e^{-i\omega h_k/\beta_k} \\ \frac{1}{2}(1-R_{k,k+1})e^{i\omega h_k/\beta_k}, & \frac{1}{2}(1+R_{k,k+1})e^{-i\omega h_k/\beta_k} \end{bmatrix} \begin{pmatrix} A_k \\ B_k \end{pmatrix}, \quad (21)$$

where A_k and A_{k+1} are the amplitudes for the upgoing waves, and B_k and B_{k+1} are those for the downgoing waves. $R_{k,k+1}$ is the impedance ratio between Layers #k and #$(k+1)$ $(= \rho_k\beta_k/\rho_{k+1}\beta_{k+1})$. Hereinafter, each component of the matrix in Equation (21) is indicated by T_{ij}^k as

$$\begin{bmatrix} T_{11}^k & T_{12}^k \\ T_{21}^k & T_{22}^k \end{bmatrix} = \begin{bmatrix} \frac{1}{2}(1+R_{k,k+1})e^{i\omega h_k/\beta_k}, & \frac{1}{2}(1-R_{k,k+1})e^{-i\omega h_k/\beta_k} \\ \frac{1}{2}(1-R_{k,k+1})e^{i\omega h_k/\beta_k}, & \frac{1}{2}(1+R_{k,k+1})e^{-i\omega h_k/\beta_k} \end{bmatrix}, \quad (22)$$

The amplitudes for Layer #k are represented by those for Layer #1 by applying Equation (21), recursively.

$$\begin{cases} A_k = T_{1i}^{k-1} \cdot T_{ij}^{k-2} \cdots T_{lm}^2 \cdot (T_{m1}^1 A_1 + T_{m2}^1 B_1) \\ B_k = T_{2i}^{k-1} \cdot T_{ij}^{k-2} \cdots T_{lm}^2 \cdot (T_{m1}^1 A_1 + T_{m2}^1 B_1) \end{cases} \quad (\text{for } k \geq 3) \quad (23)$$

$$\begin{cases} A_2 = T_{11}^1 A_1 + T_{12}^1 B_1 \\ B_2 = T_{21}^1 A_1 + T_{22}^1 B_1 \end{cases} \quad (24)$$

The traction-free condition on the free surface, $A_1 = B_1$, gives the following representation of the amplitudes:

$$\begin{cases} A_k = C_{k-1} A_1 \\ B_k = D_{k-1} A_1 \end{cases} \quad (\text{for } 1 \leq k \leq n) \quad (25)$$

$$\begin{cases} A_0 = C_n A_1 \\ B_0 = D_n A_1 \end{cases} \quad (26)$$

where C_k and D_K are defined as follows:

$$\begin{cases} C_{k-1} = T_{1i}^{k-1} \cdot T_{ij}^{k-2} \cdots T_{lm}^2 \cdot (T_{m1}^1 + T_{m2}^1) \\ D_{k-1} = T_{2i}^{k-1} \cdot T_{ij}^{k-2} \cdots T_{lm}^2 \cdot (T_{m1}^1 + T_{m2}^1) \end{cases} \quad (\text{for } k \geq 2) \quad (27)$$

$$\begin{cases} C_1 = T_{11}^1 + T_{12}^1 \\ D_1 = T_{21}^1 + T_{22}^1 \end{cases}, \quad \begin{cases} C_0 = 1 \\ D_0 = 1 \end{cases} \quad (28)$$

We introduce the identity of $C_k^* = D_k$ in the Appendix B, where C_k^* is a complex conjugate of C_k.

$P_k(\omega)$ is also defined by the square of the absolute value of A_k/A_0, as follows:

$$P_k(\omega) = \left|\frac{A_k}{A_0}\right|^2 = \frac{|C_{k-1}|^2}{|C_n|^2} \tag{29}$$

The denominator of the last part of Equation (29) is rewritten as

$$\begin{aligned} |C_n|^2 &= |T_{11}^n C_{n-1} + T_{12}^n D_{n-1}|^2 \\ &= \left|\frac{1}{2}(1+R_{n,0})\alpha_n C_{n-1} + \frac{1}{2}(1-R_{n,0})\alpha_n^* C_{n-1}^*\right|^2 \\ &= |\Re[\alpha_n C_{n-1}] + iR_{n,0}\Im[\alpha_n C_{n-1}]|^2 \\ &= (\Re[\alpha_n C_{n-1}])^2 + R_{n,0}^2(\Im[\alpha_n C_{n-1}])^2, \end{aligned} \tag{30}$$

where α_n represents the complex variables defined by $\alpha_n = e^{i\omega h_n/\beta_n}$. $\Re[\,]$ and $\Im[\,]$ indicate the real and the imaginary parts of the argument, respectively. Therefore, the average of P_1, $\langle P_1\rangle$, is represented as follows:

$$\langle P_1\rangle = \lim_{\Omega\to\infty}\frac{1}{\Omega}\int_{-\Omega/2}^{\Omega/2}\frac{d\omega}{(\Re[\alpha_n C_{n-1}])^2 + R_{n,0}^2(\Im[\alpha_n C_{n-1}])^2}. \tag{31}$$

For the two-layered case ($n = 1$), the above equation becomes Equation (13).

For the three-layered case ($n = 2$), $\alpha_2 C_1$ is a sum of periodic functions of $\omega(h_1/\beta_1 + h_2/\beta_2) = m\pi$ and $\omega(h_1/\beta_1 - h_2/\beta_2) = n\pi$ ($m, n \in \mathbb{N}$), as follows:

$$\alpha_2 C_1 = \frac{1}{2}(1+R_{1,2})e^{i\omega(h_1/\beta_1+h_2/\beta_2)} + \frac{1}{2}(1-R_{1,2})e^{-i\omega(h_1/\beta_1-h_2/\beta_2)} \tag{32}$$

If the ratio $(h_1/\beta_1 + h_2/\beta_2)/(h_1/\beta_1 - h_2/\beta_2)$ were a rational number represented by m/n ($m, n \in \mathbb{N}$), $\alpha_2 C_1$ might be a periodic function of $\omega(h_1/\beta_1 + h_2/\beta_2) = l n\pi$ ($l \in \mathbb{N}$). However, $\alpha_2 C_1$ is generally not guaranteed to be a periodic function because $(h_1/\beta_1 + h_2/\beta_2)/(h_1/\beta_1 - h_2/\beta_2)$ is a real number. Therefore, the same strategy with the two-layered case (Eq.(13)) is not applicable to cases with more than three layers ($n \geq 2$).

If the integration results become $1/R_{1,0}$, NED $\rho_1\beta_1\langle P_1\rangle$ is also equal to $\rho_0\beta_0\langle P_0\rangle$. In the same way, the average power of the upgoing waves in Layer $\#k$ ($k \geq 2$) is obtained as follows:

$$\langle P_k\rangle = \lim_{\Omega\to\infty}\frac{1}{\Omega}\int_{-\Omega/2}^{\Omega/2}\frac{(\Re[\alpha_{k-1}C_{k-2}])^2 + R_{k-1,k}^2(\Im[\alpha_{k-1}C_{k-2}])^2}{(\Re[\alpha_n C_{n-1}])^2 + R_{n,0}^2(\Im[\alpha_n C_{n-1}])^2}\,d\omega. \tag{33}$$

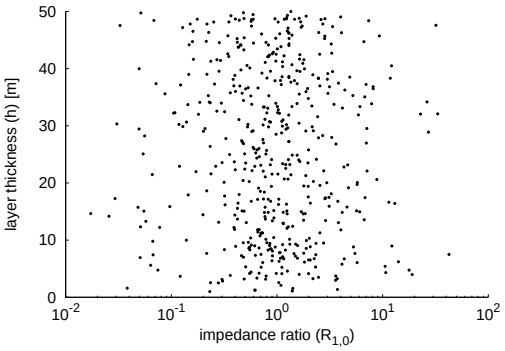

Figure 4: Parameter distribution of the impedance ratio and the layer thickness for the two-layered case.

If the integration results becomes $1/R_{k,0}$, NED is conserved through all the layers. Therefore, we apply the Monte Carlo simulation method in order to examine the conservation of NED for the cases with more than three layers in the latter chapter.

The above discussion is based on the vertical incident of SH waves. In the shallow layers of the crust structure within about 0-1000 m depth, the incident of waves from the basement is assumed to be vertical. On the other hand, the general oblique incidence of waves is also interesting. When the incident angle δ and the S-wave velocity β_k satisfy $\beta_0 > \beta_k \sin\delta$ in all layers, the problems are reduced to the same with the vertical incidence (see Appendix C).

4. Numerical tests

Firstly, the conservation of the quantity is numerically verified for the two-layered case using the Monte Carlo simulation. Five hundred sets of physical values are generated from random numbers within the range of 10-700 m/s for the S-wave velocity and 1000-2000 kg/m^3 for the density of both Layer #1 and Basement #0. The parameters set for Layer #1 are not guaranteed to be smaller than those for Basement #0 in the simulations. The layer thickness is generated within the range of 1-50 m. Figure 4 shows the parameter distribution of impedance ratio $R_{1,0}$ and layer thickness h.

For each sample, $P_1(\omega)$ is calculated by Equation (11). Figure 5 shows three samples of $P_1(\omega)$ normalized by $1/R_{1,0}$. Since the average $P_1(\omega)$ is

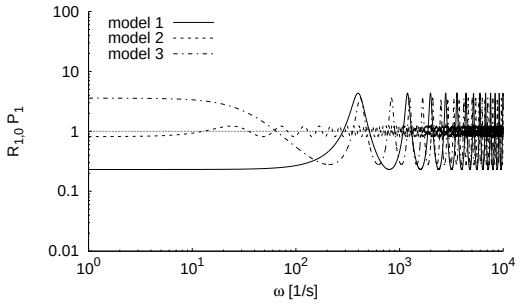

Figure 5: Samples of P_1 normalized by $1/R_{1,0}$ for the two-layered case (Model1: $R_{1,0}$=0.231, h/β_1=0.004 s, Model2: $R_{1,0}$=0.816, h/β_1=0.066 s, Model3: $R_{1,0}$=0.145, h/β_1=0.249 s).

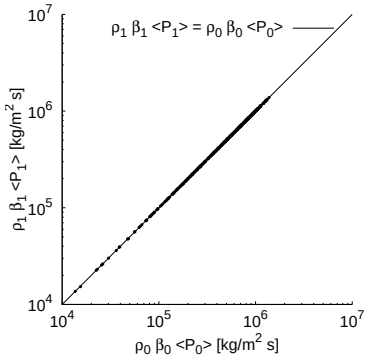

Figure 6: Comparison of NED between Layer #1 and Basement #0 for the two-layered case.

$1/R_{1,0}$, as proved in section 2, the average $R_{1,0}P_1(\omega)$ should be 1. The amplitudes and the periodicity of $R_{1,0}P_1(\omega)$ are varied among the three samples, Model 1, 2, and 3, although the values are distributed around 1.

In order to check the conservation of NED the averaged values for $\rho_1\beta_1 P_1$ are compared to those for $\rho_0\beta_0 P_0$. The integrations are approximated by a numerical integration every 1.0 s^{-1} within 1.0 $\mathrm{s}^{-1} \leq \omega \leq 2.5 \times 10^5$ s^{-1}. Figure 6 shows a comparison of NED. A line for $\rho_1\beta_1\langle P_1\rangle = \rho_0\beta_0\langle P_0\rangle$ is plotted together. The simulated samples, indicated by the black points, are exactly on the line, and thus, the conservation of NED is verified for the two-layered case.

For the three- and the four-layered cases, Monte Carlo simulations are also performed. Five hundred sets of physical values are also generated from

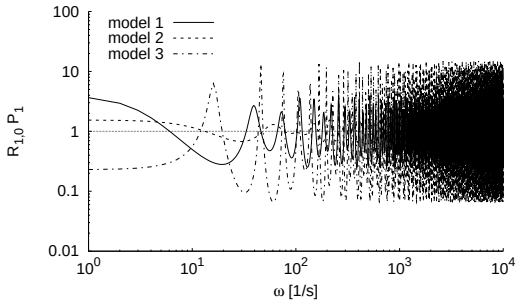

Figure 7: Samples of P_1 normalized by $1/R_{1,0}$ for the three-layered case (Model1: $R_{1,2}$=0.043, $R_{2,0}$=0.551, h_1/β_1=0.579 s, h_2/β_2=0.003 s, Model2: $R_{1,2}$=1.277, $R_{2,0}$=1.211, h_1/β_1=0.044 s, h_2/β_2=0.015 s, Model3: $R_{1,2}$=0.390, $R_{2,0}$=2.067, h_1/β_1=0.593 s, h_2/β_2=0.027 s).

random numbers within the range of 10-700 m/s for the S-wave velocity and 1000-2000 kg/m^3 for the density of every layer and for Basement #0. The total thickness of the layers is generated within the range of 1-50 m and then divided into layers with a random thickness.

Figure 7 shows three samples of $P_1(\omega)$ normalized by $1/R_{1,0}$ for the three-layered case. In section 3, we mentioned that the integration of average P_1 is not analytically discussed, although the calculated values, $R_{1,0}P_1(\omega)$, are almost distributed around 1. NED between the layers is checked in Figure 8. The integrations are also approximated by the numerical integration every 1.0 s^{-1} within 1.0 s^{-1} $\leq \omega \leq 2.5 \times 10^5$ s^{-1}. Every sample is on the reference line, and thus, NED is expected to be conserved through the layers even for the three- and the four-layered cases.

The simulations are applied to a ten-layered case. Five hundred sets of physical values are generated from the random numbers within the range of 10-700 m/s for the S-wave velocity and 1000-2000 kg/m^3 for the density of every layer and for Basement #0. The total thickness of the layers is generated within the range of 1-50 m, and then divided into layers with a random thickness. NED at Layer #1 and Basement #0 is compared in Figure 9. The integrations are approximated by a numerical integration every 0.02 s^{-1} within 0.02 s^{-1} $\leq \omega \leq 1.6 \times 10^7$ s^{-1}. Almost all the samples are on the reference line, and thus, NED is expected to be conserved between Layer #1 and Basement #0. The depth distribution of NED normalized by that of the basement, is also shown in Figure 9. The quantities are almost constant at 1 for all the layers. Therefore, the results of the Monte Carlo

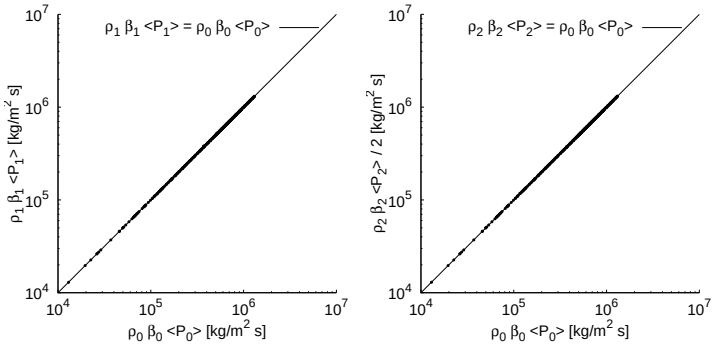

(a) three-layered case

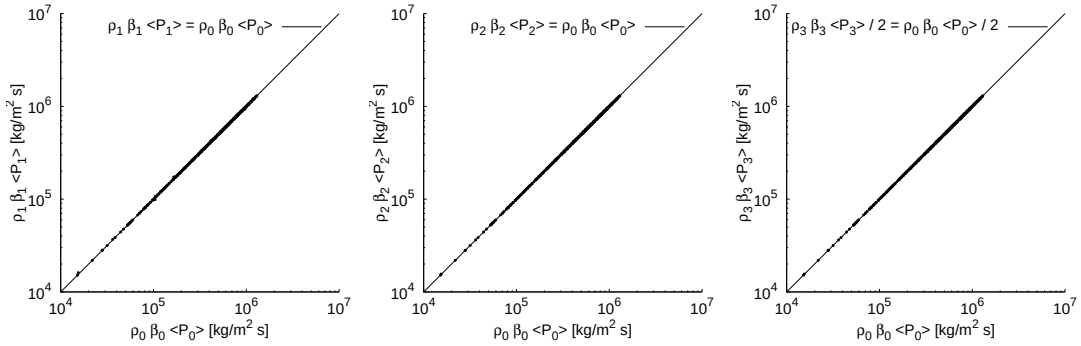

(b) four-layered case

Figure 8: Comparison of NED between Layer #1 and Basement #0 (top left) and between Layer #2 and Basement #0 (top right) for the three-layered case, and for between Layer #1 and Basement #0 (bottom left), between Layer #2 and Basement #0 (bottom middle), and between Layer #3 and Basement #0 (botom right) for the four-layered case.

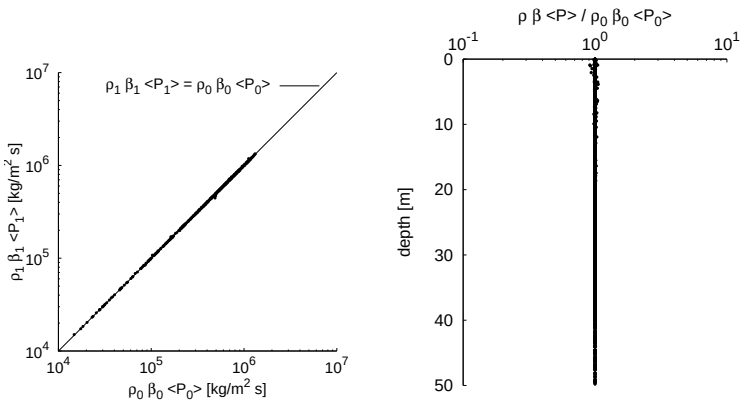

Figure 9: Comparison of NED for the ten-layered case between Layer #1 and Basement #0 (left), and depth distribution of NED normalized by NED at Basement #0 (right)

simulation support the conservation of NED through the layers.

5. Conclusions

We introduced Normalized Energy Density that is the average power for the upgoing waves multiplied by the impedance, for a 2D SH problem. For the two-layered case, the conservation of NED was analytically proved. For the three-, the four-, and the ten-layered cases, the conservation was verified by the Monte Carlo simulation method. The analytical proof for the general multi-layered case is still a problem; NED is supposed to be conserved through the layers.

We emphasize that NED can be evaluated from the transfer function and the impedance at the top layer. Detailed layered structures are not required for the evaluation. NED, different from the conventional definition of the energy, is conserved in structures whose detailed physical parameters have not been identified. It is anticipated that NED will be applied in the future to a wide range of studies. For example, a trade-off problem has been known to separate a contribution of source, pass and site effects by using the observed ground motions, e.g. Sato [9], Iwata and Irikura [10], Kinoshita [11], etc. A reference site is usually assumed to be no amplifications, and those at the other sites are estimated in terms of the ratio to the reference site. If the impedances on the free surface are known, NED constrains the average of site amplifications, and thus, the trade-offs might be avoided.

Acknowledgments

We thank the two anonymous reviewers and the editor Prof. Hailan Zhang for their thorough comments. We appreciate Prof. Francisco J. Sánchez-Sesma to have a good discussion to name the quantity Normalized Energy Density.

References

[1] A. E. H. Love, A treatise on the mathematical theory of elasticity, Dover Pubns, New York, 1927.

[2] C. Richter, An instrumental earthquake magnitude scale, Bull. Seism. Soc. Am. 25 (1935) 1–32.

[3] H. Kanamori, The energy release in great earthquakes, J. Geophys. Res. 82 (1977) 2981–2987.

[4] B. V. Kostrov, S. Das, Principles of earthquake source mechanics, Cambridge University Press, Cambridge, 1988.

[5] E. Fukuyama, Radiation energy estimated at earthquake source, Geophys. Res. Lett. 32 (2005) L13308.

[6] R. Abercrombie, A. McGarr, G. Toro, H. Kanamori, Earthquakes: radiated energy and the physics of faulting, American Geophysical Union, Washington, DC., 2006.

[7] K. Aki, P. G. Richards, Quantitativ Seismology 2nd edn, University Science Books, California, 2002.

[8] T. Kokusho, R. Motoyama, Energy dissipation in surface layer due to vertically propagating sh wave, J. Geotech. Geoenv. Eng. 128 (2002) 309–318.

[9] T. Sato, Rupture characteristics of the 1983 Nihonkai-chubu (Japan sea) earthquake as inferred from strong motion accelerograms, J. Phys. Earth. 33 (1985) 525–557.

[10] T. Iwata, K. Irikura, Source parameters of the 1983 Japan sea earthquake sequence, J. Phys. Earth. 36 (1988) 155–184.

[11] S. Kinoshita, Frequency-dependent attenuation of shear waves in the crust of the southern Kanto area, Japan, Bull. Seism. Soc. Am. 84 (1994) 1387–1396.

Appendix A. Total energy for general wave field

Let u_i displacement of a wave propagating to the direction l_i. The wave consists of both P- and S-waves.

$$u_i = u_\alpha l_i + u_{\beta 1} t_i^1 + u_{\beta 2} t_i^2, \tag{A.1}$$

where u_α is amplitude of P-wave, $u_{\beta 1}$ and $u_{\beta 2}$ are the amplitudes of S-wave in t_i^1 and t_i^2 directions, which are perpendicular to l_i. When the following identities are substituted into Eq.(1),

$$\frac{\partial u_\alpha}{\partial x_i} = -\frac{1}{\alpha}\dot{u}_\alpha l_i, \qquad \frac{\partial u_\beta}{\partial x_i} = -\frac{1}{\beta}\dot{u}_\beta l_i, \tag{A.2}$$

the total energy E is rewritten as follows:

$$E = \int_0^\infty dt \int_S \{\rho\alpha \dot{u}_\alpha^2 l_i + \rho\beta \dot{u}_\beta^2 l_i + \rho\gamma \dot{u}_\alpha \dot{u}_{\beta 1} t_i^1 + \rho\gamma \dot{u}_\alpha \dot{u}_{\beta 2} t_i^2\} n_i dS, \tag{A.3}$$

where $\gamma = \rho(\alpha + \beta - 2\beta^2/\alpha)$. Therefore the total energy E is not equal to $E_\alpha + E_\beta$, defined by Eq.(2).

Appendix B. Properties of C_k and D_k

From the definitions for C_k and D_k (Equations (27) and(28)), the following recursive formulas are obtained for $k \geq 1$.

$$\begin{cases} C_k = T_{11}^k C_{k-1} + T_{12}^k D_{k-1} \\ D_k = T_{21}^k C_{k-1} + T_{22}^k D_{k-1} \end{cases} \tag{B.1}$$

For $k = 1$, C_1 and D_1 are explicitly represented by

$$\begin{cases} C_1 = p_1 \alpha_1 + q_1 \alpha_1^* \\ D_1 = q_1 \alpha_1 + p_1 \alpha_1^* \end{cases} \tag{B.2}$$

where p_k and q_k are the real variables defined by $p_k = \frac{1}{2}(1 + R_{k,k+1})$ and $q_k = \frac{1}{2}(1 - R_{k,k+1})$, and α_k is a complex variable defined by $\alpha_k = e^{i\omega h_k/\beta_k}$.

α_k^* is the complex conjugate of α_k. Thus, D_1 is proved to be the complex conjugate of C_1.

If D_k is the complex conjugate of C_k, C_{k+1} and D_{k+1} are represented by

$$\begin{cases} C_{k+1} = p_{k+1}\alpha_{k+1}C_k + q_{k+1}\alpha_{k+1}^* D_k = p_{k+1}\alpha_{k+1}C_k + q_{k+1}(\alpha_{k+1}C_k)^* \\ D_{k+1} = q_{k+1}\alpha_{k+1}C_k + p_{k+1}\alpha_{k+1}^* D_k = q_{k+1}\alpha_{k+1}C_k + p_{k+1}(\alpha_{k+1}C_k)^* \end{cases} \tag{B.3}$$

Then, D_{k+1} becomes the complex conjugate of C_{k+1}. Therefore, C_k and D_k satisfy the following relationship proved by a mathematical induction.

$$C_n^* = D_n \tag{B.4}$$

Appendix C. Oblique incidence case

Let δ to be the incident angle of the wave propagating into Basement #0. The displacement in each layer satisfies the following wave equations:

$$-\frac{\omega^2}{\beta_k^2}u_k = \frac{\partial^2 u_k}{\partial x^2} + \frac{\partial^2 u_k}{\partial z_k^2}. \tag{C.1}$$

The general solution for the wave equation at Layer #k is obtained by

$$u_k = A_k e^{i(k_x x + k_{zk} z_k)} + B_k e^{i(k_x x - k_{zk} z_k)}, \tag{C.2}$$

where k_x and k_{zk} are the wave number in x and z_k directions, respectively. The wave numbers are related to the S-wave velocity β_k and the incident angle δ, as follows:

$$k_x = \frac{\omega \sin\delta}{\beta_0}, \qquad k_{zk} = \frac{\omega}{c_k}, \tag{C.3}$$

where c_k is the apparent S-wave velocity in z_k direction defined by,

$$c_k \equiv \beta_k \left(1 - \frac{\beta_k^2}{\beta_0^2}\sin^2\delta\right)^{-1/2}. \tag{C.4}$$

Note that c_k satisfies $\Re[c_k] > 0$ and $\Im[c_k] > 0$. When β_0 is greater than $\beta_k \sin\delta$, c_k is a real number.

From the boundary condition at the interface between Layer #$(k+1)$ and #k, the amplitudes for Layer #$(k+1)$ are represented by those for Layer #k as

$$\begin{pmatrix} A_{k+1} \\ B_{k+1} \end{pmatrix} = \begin{bmatrix} \frac{1}{2}(1+\tilde{R}_{k,k+1})e^{i\omega h_k/c_k}, & \frac{1}{2}(1-\tilde{R}_{k,k+1})e^{-i\omega h_k/c_k} \\ \frac{1}{2}(1-\tilde{R}_{k,k+1})e^{i\omega h_k/c_k}, & \frac{1}{2}(1+\tilde{R}_{k,k+1})e^{-i\omega h_k/c_k} \end{bmatrix} \begin{pmatrix} A_k \\ B_k \end{pmatrix}, \tag{C.5}$$

where $\tilde{R}_{k,k+1}$ is defined by

$$\tilde{R}_{k,k+1} \equiv \frac{\rho_k \beta_k^2 / c_k}{\rho_{k+1} \beta_{k+1}^2 / c_{k+1}}. \tag{C.6}$$

The above system of equations are the same form with Eq.(21). When c_k is a real number in each layer, $\tilde{R}$ becomes a real number, and $e^{i\omega h_k/c_k}$ and $e^{-i\omega h_k/c_k}$ are complex numbers with the absolute values of 1. In the case, $\langle P_k \rangle$, defined by $\langle |A_k/A_0|^2 \rangle$, is the same with Eq.(33) if impedance and S-wave velocity are exchanged to $\rho_k \beta_k^2/c_k$ and c_k, respectively. Therefore, the oblique incident case is identical to the problems of vertical incidence with the impedance of $\rho_k \beta_k^2/c_k$ and S-wave velocity of c_k if $\beta_0 > \beta_k \sin\delta$ is satisfied in each layer.